Proceedings of the 13th
IEEE International Conference on Nanotechnology
Beijing, China, August 5-8, 2013

An Inter-Segment Tunneling Nanoscale Force Sensor: Modeling and Simulation

Gautham Dharuman, Zheng Fan, *Student Member, IEEE,* and Lixin Dong*, *Senior Member, IEEE*

Department of Electrical and Computer Engineering, Michigan State University, East Lansing, MI 48824, USA
*Email: ldong@egr.msu.edu

***Abstract*— A segmented high aspect ratio nanowire employing the tunneling effect is proposed to theoretically realize non-linear effects in nanoscale force sensing. The structure consists of an external insulating shell with metallic core regions separated at the structure's geometric center. The separation is considered to be in the order of a few Å for the tunneling effect to be pronounced. As the structure is subjected to an axial force at the ends, buckling occurs causing a change in the separation which results in a non-linear change in the current. Force-separation and current-force relations are studied and the high sensitivity of the structure as a force sensor is established.**

Index terms- segmented, force sensor, tunneling effect, buckling, sensitivity

I. Introduction

Nanoscale force sensors are finding widespread applications in biological force sensing [1] where the forces involved range from a few picoNewtons (pNs) to tens of nanoNewtons (nNs). Sensitivity of force measurement is of vital importance when small changes in force are to be detected. For example, changes in force as a RNA molecule unzips could only be a fraction of the initial force [2]. Sensors with non-linear monotonic increase in output signal with increasing force are required to realize such high sensitivities. Piezoelectric nanowire force sensors despite their merits cannot be employed due to the linear current-force variation. Sensing based on tunneling effect could serve the purpose due to exponential dependence on barrier height and width. A nanoscale force sensor based on the piezotronic effect [3] has a non-linear variation. The effect is based on tunneling current between a metallic atomic force microscope (AFM) tip and a semiconducting nanowire which restricts sensing to metallic objects if the nanowire is used as the probe. This constraint is overcome by the inter-segment structure which employs the tunneling effect between embedded metallic regions and therefore force transduction is independent of the electrical property of the object being sensed. Being compact with the tunneling junction in-built, the device would be free of alignment requirements which is an issue in case of scanning tunneling microscope (STM) based force sensors (another class of sensors that employ the tunneling effect) that limits their performance and application.

II. Modeling

The model is composed of two parts – a mechanical model to determine the relation between the force and the separation and a tunneling model to obtain the current for the corresponding change in separation. The two models are then combined to determine the relation between the force and the current. The proposed structure and the separation change with application of force are schematically shown in Fig. 1. An expanded view of the separation is shown in Fig. 2.

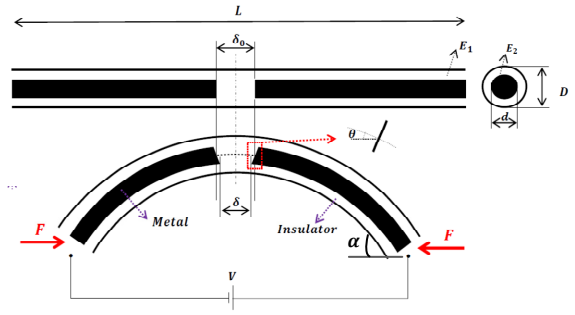

Fig. 1 Proposed structure and the decrease in separation as the nanowire is subjected to external buckling force. E_1 and E_2 are the Young's modulus of the insulating and metallic regions respectively; δ_0 is the initial separation between the metallic regions; δ is the separation between the lower edges, θ is the angle of rotation of the plane of the metallic region and α is the terminal deflection angle under the action of force; D and d are the outer and inner diameters of the core-shell structure.

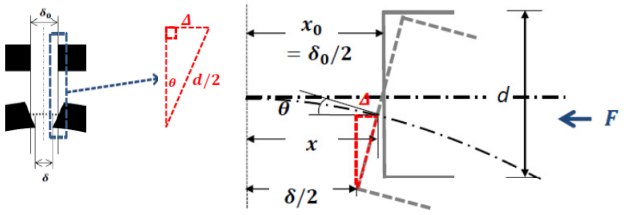

Fig. 2 An expanded schematic for the geometric analysis to obtain relation between separation and angle of rotation.

From the figure the relation between the separation δ, the angle of rotation θ and the x coordinate of the point of intersection between the plane and the deformed axis can be expressed as

Authorized licensed use limited to: University of Houston. Downloaded on May 31,2023 at 13:18:13 UTC from IEEE Xplore. Restrictions apply.

$$\delta = 2x - d\ sin\theta \tag{1}$$

The separation is then correlated with the force F through the equation for axial curvature which relates θ and x with F. From the Euler-Bernoulli beam theory for buckling [4, 5], the relation between curvature and force is given by

$$\frac{d\theta}{ds} = \sqrt{\frac{2F}{EI}}\sqrt{cos\theta - cos\alpha} \tag{2}$$

where E is the Young's modulus of the nanowire, I is the area moment of inertia and α is the terminal deflection angle as shown in Fig. 1. Using (2) and the condition that the length of the axis remains unchanged for pure buckling [6], θ can be related to F through the initial axial separation δ_0 between the metallic regions resulting in the relation

$$\delta_0 = \sqrt{\frac{EI}{F}}F_e(\theta, \alpha) \tag{3}$$

where $F_e(\theta, \alpha)$ is the incomplete elliptic integral of the first kind [7] which is a function of α and θ. Assuming that δ_0 is a known value, θ can be obtained by inverting F_e for a given α. This is done through the Jacobian elliptic sine function $sn(u)$ [7], where $u = F_e(\theta, \alpha) = \sqrt{\frac{F}{2EI}}\delta_0$. The angle of rotation is then obtained as

$$\theta = 2\ sin^{-1}(sin(\alpha/2)sn(u)) \tag{4}$$

x is obtained from (2) using the relation $dx = ds\ cos\theta$ to give

$$x = \left[\sqrt{\frac{EI}{F}}\ (2\ E(\theta, \alpha))\right] - \frac{\delta_0}{2} \tag{5}$$

where $E(\theta, \alpha)$ is the incomplete elliptic integral of the second kind [7]. Since (4) and (5) involve α, the correlation between force and the separation δ would be complete if a relation between α and force is obtained. This is obtained by once again making use of the condition that the axial length remains unchanged for pure buckling leading to

$$l = \sqrt{\frac{EI}{F}}K(\alpha) \tag{6}$$

where $K(\alpha)$ is the complete elliptic integral of the first kind [7] and l is the half length of the nanowire. Inverting $K(\alpha)$ gives the relation between the force and α. Therefore, using (4), (5) and (6) in (1) the relation between separation and force can be obtained numerically. The separation δ between the lower edges was of interest because the tunneling current would be along this path which is the least distance path between the metallic regions. This is also referred to as the 'least action path' or the 'maximum probability path' for tunneling [8, 9]. The current through this path is obtained using the metal-insulator-metal tunneling junction model [10]. Since only structural enhancement to the tunneling current is of interest, a low bias condition across the junction is considered which gives the relation between the current and the separation as

$$I = I_0 \exp\left(-\frac{4\pi\delta}{h}\sqrt{2m\phi_0}\right) \tag{7}$$

where I_0 is a prefactor, h is the Planck's constant, m is the electron mass and ϕ_0 is the equilibrium barrier height as shown in Fig. 3.

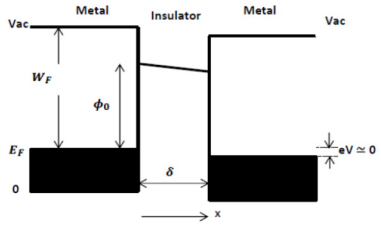

Fig. 3 Potential profile of the metal-insulator-metal junction under the application of a low bias V. ϕ_0 is the equilibrium barrier height. E_F and W_F are the Fermi energy and the work function of the metal respectively.

Though the separation-current relation is analytical (7), the relation between separation and force involves several complicated mathematical functions and operations which make it difficult to acquire a physical understanding of the effect of force on separation and thereby the tunneling current. A closed form relation between separation and force would be useful in this regard. This involves studying the numerical results (described in the next section) for different cases to come to a conclusion that x does not deviate much from x_0 and (6) and (4) could be inverted using series expansion in the limit of small α [11]. In this limit, if only linear terms of the series are retained

$$K(\alpha) \sim \frac{\pi}{2}\left(1 + sin(\alpha/2)\right)$$
$$sn\ (u) \sim \sin\ (u) \tag{8}$$

The approximate expression for δ in this limit is given by

$$\delta \sim \delta_0 - 2d\ sin(\theta/2) \tag{9}$$

Using (4), (6) and (8) in (9) results in the closed form relation between separation and force

$$\delta \sim \delta_0 - 2d\left(\frac{8}{\pi}\sqrt{\frac{F}{EI}}l - 4\right) sin\left(\sqrt{\frac{F}{EI}}\frac{\delta_0}{2}\right) \tag{10}$$

In addition to providing a direct relation this closed form expression is significant for understanding and quantifying the influence of the mechanical and geometrical parameters on the separation-force relation. Moreover, to include the effect of the different mechanical properties of the metallic regions, the flexural rigidity EI is replaced by a combined flexural rigidity which takes the form

$$(EI)_c = E_1I_1 + E_2I_2 = \frac{\pi E_1(D^4 - d^4)}{4} + \frac{\pi E_2 d^4}{4} \tag{11}$$

Authorized licensed use limited to: University of Houston. Downloaded on May 31,2023 at 13:18:13 UTC from IEEE Xplore. Restrictions apply.

III. Results and Discussion

Following are the parameters used for the simulation: Young's modulus of the shell and core are E_1 = 100 GPa, E_2 = 50 GPa respectively; equilibrium barrier height ϕ_0 = 1 eV; applied voltage 0.2 V; length of the nanowire L = 800 nm; outer diameter D = 20 nm; inner diameter d = 7.5 nm; separation before deformation δ_0 = 1nm. The separation-force curve is first numerically obtained and the result is as shown in Fig. 4(a). A non-linear drop is observed. Correspondingly, a highly non-linear rise in current with increasing force is found as shown in Fig. 4b. The rise is faster than an exponential increase as is evident from the log(current)-force relation (Fig. 4(b): inset(i)). This is due to the drop in separation with force that is faster than an exponential decline (Fig. 4(a): inset(ii)). The shape of the force-separation curve can be easily understood from the closed form expression (10) which indicates that the separation approximately drops as $\sqrt{F}$ for initial force range which corresponds to small deflection angles (α).

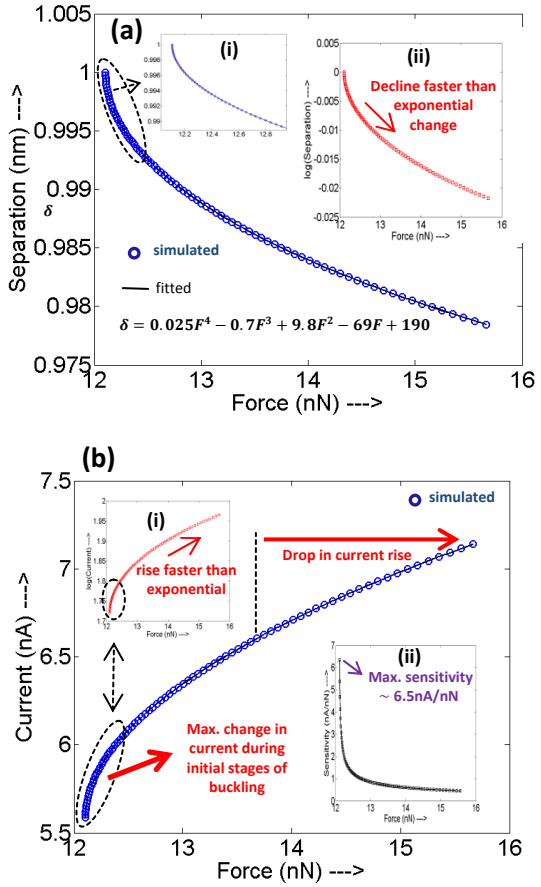

Fig. 4 (a) Separation vs. force with fitted equation, (i) force range corresponding to max. decrease in separation, (ii) log(separation) vs. force. (b) Current vs. force, (i) log(current) vs. force, (ii) Sensitivity vs. force.

It is evident that the max. current change occurs during the initial stages of buckling resulting in an enormous sensitivity $\left(\frac{\Delta I}{\Delta F}\right)$ of about 6.5 nA/nN (Fig. 2(b): inset(ii)) implying a current rise of 65pA for every 10pN rise in force value. This reflects a higher resolution in force sensing as compared to [3] which works only for a transverse bending force. For the inter segment structure, in addition to axial force, separation change can also be effected by a transverse force. Versatility in sensing is therefore implicit. Although the sensitivity for this structure is found to have a non-linear curve, a specific region can be selected from the force range depending on the application and the corresponding sensitivity variation could be linearized. The closed form expression (10) also provides explanation for the non-zero initial force and the extent of decrease in separation. The initial force is non-zero because δ equals the initial value δ_0 when

$$F = \frac{\pi^2 EI}{4l^2} = F_{cr} \tag{12}$$

which is referred to as the critical force [4-6], i.e., the minimum force required to induce buckling and hence cause change in separation. Since current enhancement needs to be pronounced, greater reduction in separation is required. For the same nanowire this can be achieved by reducing the length while keeping all other parameters fixed. The effect of reducing the length to one-fourth of its original value is shown in Fig. 5. The reduction in separation is from 1 to 0.92 nm as compared to the reduction from 1 to 0.98 nm for the initial case (Fig. 2(a)). This can also be easily understood from (10) – smaller length implies greater critical force hence much larger force values are required to cause the same deflection thereby resulting in much greater reduction in the separation.

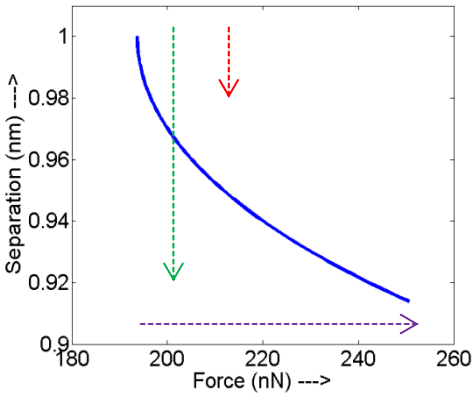

Fig. 5 Greater reduction in separation with a simultaneous shift in the critical force and increased force range compared to the result in Fig. 2(a).

Simulations were also carried out for different inner and outer diameters to understand their effect on sensitivity. Current density-force plot for fixed outer diameter (D =20nm) and different inner diameters (d=7, 7.5 and 8nm) is shown in Fig. 6. An interesting cross over region is evident (Fig. 6: inset(i)). Also shown is the corresponding

Authorized licensed use limited to: University of Houston. Downloaded on May 31,2023 at 13:18:13 UTC from IEEE Xplore. Restrictions apply.

separation-force plot (Fig. 6: inset(ii)). The cross over region is as a result of the combined flexural rigidity (11).

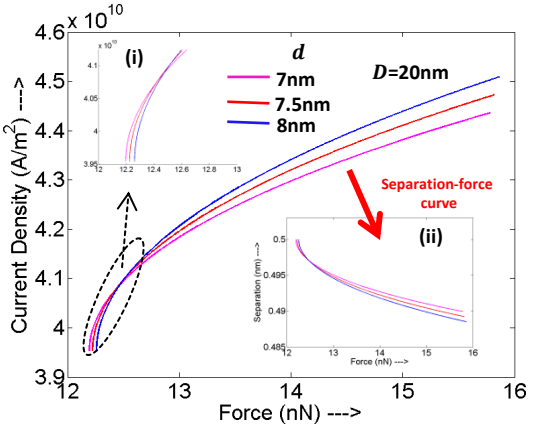

Fig. 6 Current density-force variation for fixed outer diameter D and different inner diameters d, (i) expanded cross over region, (ii) corresponding separation-force variation.

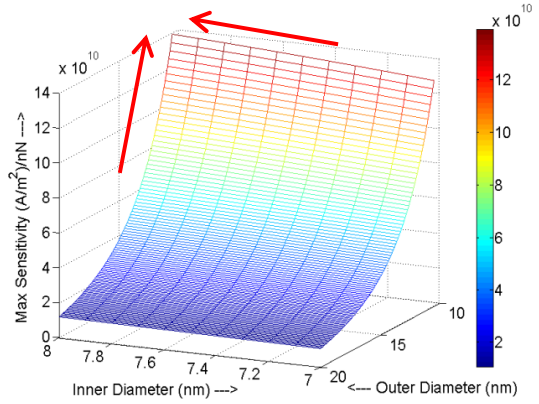

Fig. 7 Surface plot showing variation of maximum sensitivity for different inner and outer diameters for the shell-core structure.

Below the cross over point the increase in current density is found to be greater for the structure with smaller inner diameter (Fig. 6: inset(i)) which seems surprising since the opposite effect is expected based on (1). However, this can be understood in terms of the critical force (12) which is smaller for smaller inner diameter (due to reduced combined flexural rigidity). Beyond the cross over point, the bigger inner diameter structure causes a greater rise in current which is understood from (1). The effect of varying both inner and outer diameters is revealed in the surface plot shown in Fig. 7. From the figure it is evident that the structure with smaller inner and outer diameters has the maximum sensitivity. This can be understood from the previous discussions. Analysis of the current-force and the sensitivity relations for small difference in inner diameter dimensions is significant when an array of these structures is used for collective sensing. As shown, a difference of even 5 Ang. has a tremendous effect on the sensitivity and could therefore result in measurement errors that can be understood from this model.

IV. Conclusions

A tunneling effect based nanoscale force sensor for high resolution force sensing is proposed. Current-force relations and the corresponding sensitivities were studied. Results show the desired faster than exponential variation. In addition are the merits of compact and alignment free aspects of the design. A closed form expression is obtained which facilitates a physical understanding of the decrease in separation with increasing force and the influence of mechanical and geometrical parameters on this reduction. As an initial step towards design optimization, the effect of core-shell diameters and their Young's moduli on the maximum sensitivity is also studied.

Acknowledgement

This work is supported by the NSF (IIS-1054585) .

References

[1] S. J. Koch, G. E. Thayer, A. D. Corwin, and M. P. de Boer, "Micromachined piconewton force sensor for biophysics investigations," *Applied Physics Letters,* vol. 89, art. no. 173901, Oct 2006.

[2] S. Mogurampelly, S. Panigrahi, D. Bhattacharyya, A. K. Sood, and P. K. Maiti, "Unraveling siRNA unzipping kinetics with graphene," *Journal of Chemical Physics,* vol. 137, art. no. 054903, Aug 2012.

[3] Y. S. Zhou, R. Hinchet, Y. Yang, G. Ardila, R. Songmuang, F. Zhang, Y. Zhang, W. H. Han, K. Pradel, L. Montes, M. Mouis, and Z. L. Wang, "Nano-newton transverse force sensor using a vertical GaN nanowire based on the piezotronic effect," *Advanced Materials,* vol. 25, pp. 883-888, Feb 2013.

[4] G. F. Wang and X. Q. Feng, "Surface effects on buckling of nanowires under uniaxial compression," *Applied Physics Letters,* vol. 94, art. no. 141913, Apr 2009.

[5] C.-L. Hsin, W. Mai, Y. Gu, Y. Gao, C.-T. Huang, Yuzi Liu, L.-J. Chen, and Z.-L. Wang, "Elastic properties and buckling of silicon nanowires," *Advanced Materials,* vol. 20, pp. 3919-3923, 2008.

[6] S. P. Timoshenko and J. M. Gere, *Theory of Elastic Stability*. New York: McGraw-Hill, 1985.

[7] T. F. Lemczyk and M. M. Yovanovich, "Efficient evaluation of incomplete elliptic integrals and functions," *Computers & Mathematics with Applications,* vol. 16, pp. 747-757, 1988.

[8] R. Nandkishore and L. Levitov, "Common-path interference and oscillatory Zener tunneling in bilayer graphene p-n junctions," *Proceedings of the National Academy of Sciences of the United States of America,* vol. 108, pp. 14021-14025, Aug 2011.

[9] T. Taketsugu and K. Hirao, "A least-action variational method for determining tunneling paths in multidimensional system," *Journal of Chemical Physics,* vol. 107, pp. 10506-10514, Dec 1997.

[10] J. G. Simmons, "Generalized formula for the electric tunnel effect between similar electrodes separated by a thin insulating film," *Journal of Applied Physics,* vol. 34, pp. 1793-1803, 1963.

[11] A. Schett, "Properties of the Taylor series expansion coefficients of the Jacobian elliptic functions," *Mathematics of Computation,* vol. 30, pp. 143-147, 1976.

Authorized licensed use limited to: University of Houston. Downloaded on May 31,2023 at 13:18:13 UTC from IEEE Xplore. Restrictions apply.